J. Biochem. 129, 373–382 (2001)

Surface Dynamics of Bacteriorhodopsin as Revealed by ^{13}C NMR Studies on [^{13}C]Ala-Labeled Proteins: Detection of Millisecond or Microsecond Motions in Interhelical Loops and C-Terminal α-Helix[1]

Satoru Yamaguchi,* Satoru Tuzi,* Koka Yonebayashi,* Akira Naito,* Richard Needleman,† Janos K. Lanyi,‡ and Hazime Saitô*,[2]

*Department of Life Science, Faculty of Science, Himeji Institute of Technology, Harima Science Garden City, Kouto 3-chome, Kamigori, Hyogo 678-1297; †Department of Biochemistry, Wayne State University, Detroit, Michigan 48201, USA; and ‡Department of Biophysics and Physiology, University of California, Irvine, California 92697-4560, USA

Received October 16, 2000; accepted December 11, 2000

We have recorded ^{13}C NMR spectra of [2-^{13}C]-, [1-^{13}C]-, [3-^{13}C],- and [1,2,3-$^{13}C_3$]Ala-labeled bacteriorhodopsin (bR), and its mutants, A196G, A160G, and A103C, by means of cross polarization-magic angle spinning (CP-MAS) and dipolar decoupled-magic angle spinning (DD-MAS) techniques, to reveal the conformation and dynamics of bR, with emphasis on the loop and C-terminus structures. The ^{13}C NMR signals of the loop (C-D, E-F, and F-G) regions were almost completely suppressed from [2-^{13}C]-, [1-^{13}C]Ala-, and [1-^{13}C]Gly-labeled bR, due to the presence of conformational fluctuation with correlation times of 10^{-4} s that interfered with the peak-narrowing by magic angle spinning. The observation of such suppressed peaks for specific residues provides a unique means of detecting intermediate frequency motions on the time scale of ms or μs in the surface loops of membrane proteins. Instead, the three well-resolved ^{13}C CP-MAS NMR signals of [2-^{13}C]Ala-bR, at 50.38, 49.90, and 47.96 ppm, were ascribed to the C-terminal α-helix previously proposed from the data for [3-^{13}C]Ala-bR: the former two peaks were assigned to Ala 232 and 238, in view of the results of successive proteolysis experiments, while the highest-field peak was ascribed to Ala 235 prior to Pro 236. Even such ^{13}C NMR signals were substantially broadened when ^{13}C NMR spectra of fully labeled [1,2,3-^{13}C]Ala-bR were recorded, because the broadening and splitting of peaks due to the accelerated transverse relaxation rate caused by the increased number of relaxation pathways through a number of ^{13}C-^{13}C homo-nuclear dipolar interactions and scalar J couplings, respectively, are dominant among ^{13}C-labeled nuclei. In addition, approximate correlation times for local conformational fluctuations of different domains, including the C-terminal tail, C-terminal α-helix, loops, and transmembrane α-helices, were estimated by measurement of the spin-lattice relaxation times in the laboratory frame and spin-spin relaxation times under the conditions of cross-polarization-magic angle spinning, and comparative study of suppressed specific peaks between the CP-MAS and DD-MAS experiments.

Key words: bacteriorhodopsin, C-terminal α-helix, interhelical loops, membrane proteins, surface dynamics.

Bacteriorhodopsin (bR) is a light-driven proton pump in the purple membrane from *Halobacterium salinurum* consisting of seven transmembrane α-helices linked to the chromophore at Lys 216. Its three-dimensional structures in the ground state as well as the photolyzed state have been recently revealed by several laboratories, utilizing cryo-electron microscopy (*1–3*) or X-ray diffraction (*4–10*), as far as the structure of the transmembrane helices and some loops are concerned. No consistent data, however, are available, including of several residues missing from the revealed structures of N- or C-terminus and some interhelical loops. This is probably because these portions of bR are rather more flexible than anticipated and their structures could be altered under the crystallization conditions. It seems to be important to obtain a more detailed picture of surface residues, such as interhelical loops, in view of their participation in, for instance, the conformational switch during photocycles. This is true for the C-terminus, although they are not always believed to play an important role in the photocycles of bR (*11*). Nevertheless, a more detailed picture of surface residues is worthwhile obtaining, when one takes bR into account as a prototype of a number of membrane proteins involved in a variety of signal transduction in G-protein coupled receptors.

[1] This work has been supported, in part, by Grants-in-Aid for Scientific Research (09480179 and 09558094) from the Ministry of Education, Science, Sports and Culture of Japan.

[2] To whom correspondence should be addressed. Tel: +81-791-58-0181, Fax: +81-791-58-0182, E-mail: saito@sci.himeji-tech.ac.jp

Abbreviations: bR, bacteriorhodopsin; CP-MAS, cross polarization-magic angle spinning; DD-MAS, dipolar decoupled-magic angle spinning.

© 2001 by The Japanese Biochemical Society.

Fluorescence (*12*, *13*), spin- (*14*), and heavy atom-labeling (*15*, *16*) techniques have been utilized to examine the conformational features of the C-terminus and loop regions, even though these probes are not always free from perturbation due to steric hindrance by the introduced probes. We have therefore explored a ^{13}C NMR approach to reveal the conformation and dynamics of ^{13}C-labeled membrane proteins with reference to the conformation-dependent displacements of ^{13}C chemical shifts (*17–19*). We have so far utilized [3-^{13}C]alanine as a source of ^{13}C-labeling to probe backbone conformations, in spite of the location of the label on its side-chain, mainly because displacements of ^{13}C NMR signals of this label are solely dependent on the local conformation of the peptide unit, as defined by a set of the torsion angles (ϕ and ψ) not affected by hydrogen bonds, as in the case of C_α and carbonyl carbons (*17*, *20*), and plausible scrambling of isotopes to other residues turned out to be minimal (*20*). Dynamic aspects of protein backbones can now be determined from measurements of a variety of relaxation parameters, once ^{13}C NMR signals have been correctly assigned to specific amino acid residues on the basis of the conformation-dependent displacements of peaks. In fact, the existence of the C-terminal α-helix (226–235) protruding from the membrane surface was proposed on the basis of the ^{13}C NMR signals of Ala 228 and 230 with reference to the standard value, together with the assignment of peaks to the transmembrane α-helices and loops (*21–23*). In addition, it should emphasized that a certain area of ^{13}C NMR signals could be suppressed either from CP-MAS or both CP-MAS and DD-MAS NMR spectra, when the peak-narrowing by proton-decoupling or magic angle spinning fails due to interference with incoherent motions of conformational fluctuations, especially at physiological temperature (*23–25*). It seems worthwhile to extend this approach to [2-^{13}C]-, [1-^{13}C]-, or [1,2,3-$^{13}C_3$]Ala-bR, because the correlation times of motions responsible for such peak-suppression are obviously different in view of the respective relaxation mechanism (*24*).

The present study was therefore undertaken to further elucidate the conformation and dynamics of the surface domains of bR, including the C-terminal tail, C-terminal α-helix and interhelical loops, by comparative ^{13}C NMR studies on [1-^{13}C]-, [2-^{13}C]-, or [1,2,3-$^{13}C_3$]Ala-labeled bR. The existence of the C-terminal α-helix protruding from the membrane surface was first confirmed on the basis of the conformation-dependent ^{13}C chemical shifts of the [2-^{13}C]Ala residue and the spin-lattice relaxation times. Unexpectedly, the ^{13}C NMR signals of the loop regions of [2-^{13}C]Ala-bR were completely suppressed, although these signals of [3-^{13}C]Ala-bR were easily visible (*21*, *23*, *25*). This finding unequivocally leads to arriving at the conclusion that the looped structure is not static as anticipated, but is in a time-

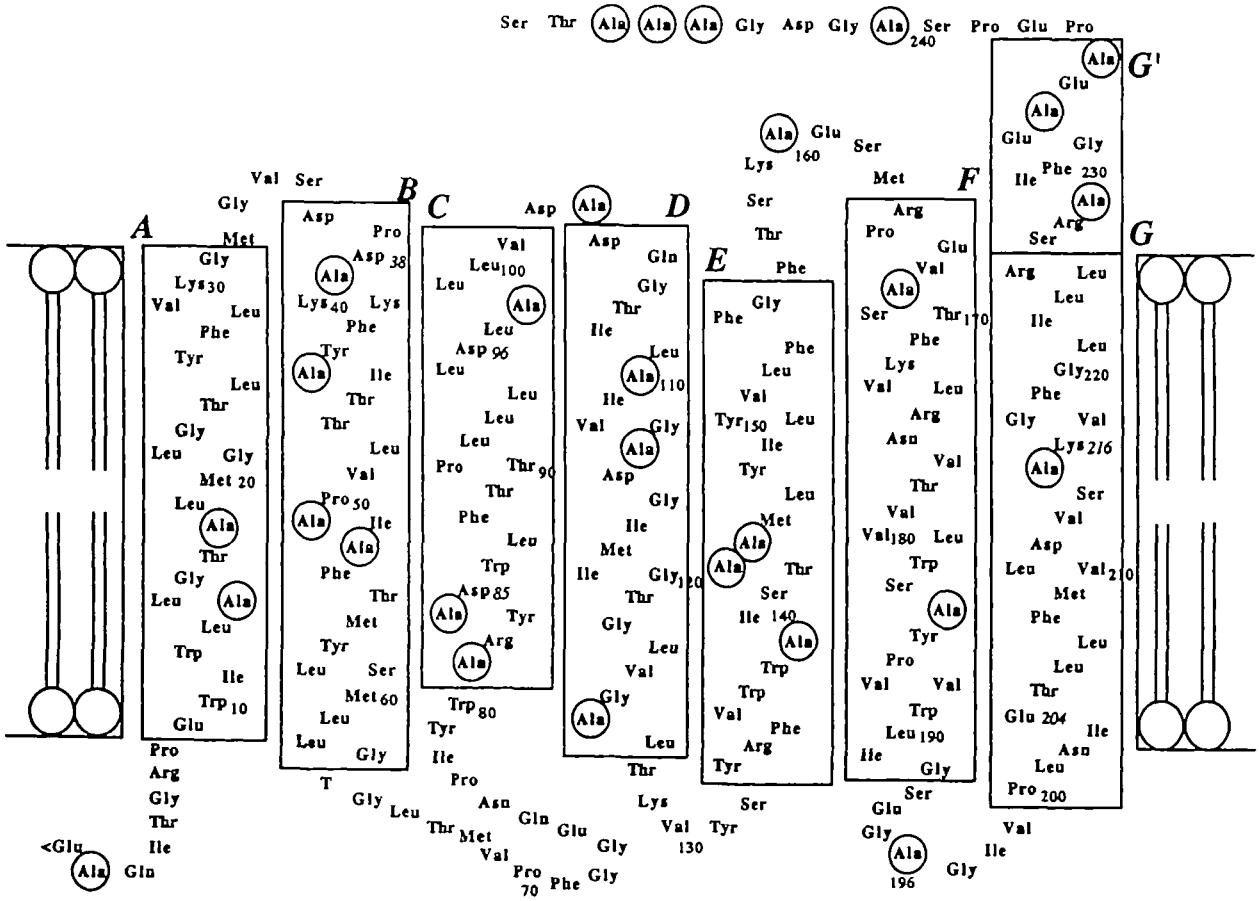

Fig. 1. **Schematic representation of the secondary structure of bacteriorhodopsin.** All Ala residues are circled. The locations of transmembrane helices A–G in the boxes are based on the X-ray diffraction results of Luecke *et al.* (*7*). The presence of helix G' protruding from the membrane surface is based on our previous NMR data (*23*).

averaged state undergoing conformational fluctuation with a correlation time in the order of 10^{-4} s, which could be interfered with the magic angle spinning frequency responsible for the averaging of the chemical shift anisotropy of C_α and carbonyl carbons. The biological significance of such flexibility of the interhelical loops will be discussed as to a hinge allowing large amplitude movements of the transmembrane α-helices during the photocycles. In addition, it was found that much broadened spectral lines were observed when fully ^{13}C-labeled proteins were prepared, because the transverse relaxation rates were substantially increased in the presence of an increased number of relaxation pathways through a number of homonuclear dipolar interactions.

MATERIALS AND METHODS

Sample Preparation—L-[1-^{13}C]-, L-[2-^{13}C]-, L-[3-^{13}C]alanine, and [1-^{13}C]glycine were purchased from CIL, Andover, MA, and used without further purification. L-[1,2,3-$^{13}C_3$]alanine was purchased from ICON Stable Isotopes, NY, USA. *H. salinarum* strain S9 was grown in the TS medium of Onishi *et al.* (*26*), in which unlabeled L-alanine or glycine was replaced by one of the above-mentioned ^{13}C-labeled amino acids. Site-directed mutants, A103C, A160G, and A196G in the C-D, E-F, and F-G loops, respectively (Fig. 1), were also ^{13}C-labeled with the above-mentioned amino acid residues by means of this biosynthesis. In Fig. 1, the presence of the two turn α-helix revealed by a ^{13}C NMR study (*21–23*) is illustrated as the G′ helix, protruding from the membrane surface. Purple membranes were isolated by the method of Oesterhelt and Stoeckenius (*27*), and suspended in 5 mM HEPES buffer containing 0.02% NaN_3 and 10 mM NaCl, pH 7, unless otherwise mentioned. Proteolysis with carboxypeptidase A and papain was carried out as described by Liao and Khorana (*11*). The samples were concentrated by centrifugation and the pelleted preparations thus obtained were placed in a 5 mm o.d. zirconia pencil-type rotor. A teflon cap was tightly glued to the rotor to prevent dehydration through a pin-hole in the cap during magic angle spinning under a stream of dried compressed air.

Measurement of ^{13}C NMR Spectra—100.7 MHz high-resolution solid-state NMR spectra were recorded in the dark with a Chemagnetics CMX-400 NMR spectrometer, both CP-MAS or DD-MAS with a single pulse excitation method. The spectral width and contact time, and repetition and acquisition times for CP-MAS NMR were 40 kHz, 1 ms, 4 s, and 50 ms, respectively. The $\pi/2$ pulses for carbon and proton nuclei were 5 μs, and the spinning rate was 3 kHz. Free induction decays were acquired with data points of 2K. Fourier transformation was carried out as 16K points after 14K points were zero-filled. The carbon spin-lattice relaxation times in the laboratory frame (T_1^C) were measured by the cross polarization enhancement procedure with reversal of spin-temperature or standard inversion recovery using either the CP-MAS or DD-MAS NMR techniques, respectively. Spin-spin relaxation times under the conditions for proton decoupling and magic angle spinning (T_2^C) were measured using a Hahn spin echo pulse sequence, adjusting the interval between the π pulse and the starting point of acquisition to a multiple of the rotor period N_cT_r in the usual manner (*28*). ^{13}C chemical shifts were referred to the chemical shifts of the carboxyl carbon of glycine [176.03 ppm from tetramethylsilane (TMS)], and converted to data relative to TMS. All NMR spectra were recorded at 20°C with the passage of air through the thermostated coolant.

RESULTS

Figure 2 illustrates the ^{13}C NMR spectra of [2-^{13}C]Ala-bR, recorded by both the DD-MAS (A) and CP-MAS (B) methods. The ^{13}C NMR signals of the C_α carbons in the transmembrane α-helices are displaced downfield as compared with those of turned structures located in the loops, as illustrated in the top trace, with reference to the previous data for a number of model polypeptides (*18, 19*). Surprisingly, only two broad signals, at 53.2 and 51.6 ppm, were resolved for the transmembrane α-helical regions of [2-^{13}C]Ala-bR in the ^{13}C CP-MAS NMR spectrum (Fig. 2B), in contrast to the nine resolved signals from [3-^{13}C]Ala-bR in this region previously reported (*29*). The intense signal present at 50.1 ppm on DD-MAS NMR is ascribed to Ala 240, 244–246 in the terminal tail of the C-terminus undergoing conformational fluctuation, taking on the random coil conformation, with reference to the C_α ^{13}C chemical shift of the random coil form at 50.1 ppm (*23*), because the corresponding [3-^{13}C]Ala peak was also suppressed in the CP-MAS NMR spectra of [3-^{13}C]Ala-bR (*21, 30*).

Unexpectedly, no spectral change was observed when the ^{13}C CP-MAS (A-D) and DD-MAS (E-H) NMR spectra of the wild type and three types of site-directed mutants, A103C, A160G, and A196G, were compared, with the expectation of being able to assign the C_α ^{13}C NMR signals of Ala 103, 196, and 160, respectively, as a peak with reduced peak-intensity, as illustrated in Fig. 3. This finding implies that the ^{13}C NMR signals of these loops of [2-^{13}C]Ala-bR were completely suppressed in both the CP-MAS and DD-MAS NMR spectra, although the corresponding ^{13}C NMR signals of [3-^{13}C]Ala-bR were well-resolved and the ^{13}C signals of

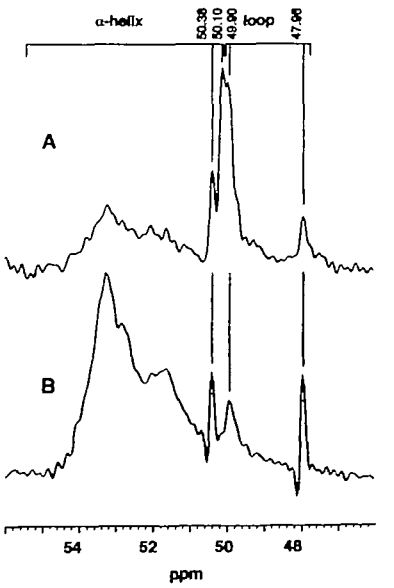

Fig. 2. 100.7 MHz ^{13}C DD-MAS (A) and CP-MAS (B) NMR spectra of [2-^{13}C]Ala-labeled bacteriorhodopsin.

Ala 196, 103, *etc.* were appreciably suppressed for the respective site-directed mutants, A196G, A103C, *etc.*, as demonstrated previously (*25*, *29*).

Instead, these well-resolved ^{13}C DD-MAS NMR signals resonating at the peak-positions of the loop region (Figs. 2 and 3) may arise from the Ala residues located in the C-terminus undergoing more rapid conformational fluctuation. To prove this, the ^{13}C NMR spectra obtained by the CP-MAS (A-C) and DD-MAS (D-F) methods were compared after successive limited proteolysis with carboxypeptidase A (B and E) and papain (A and D), as shown in Fig. 4. Obviously, the remaining single ^{13}C NMR signal of the papain-treated preparation (Fig. 4, A and D) resonating at 50.03 ppm can be straightforwardly ascribed to Ala 228, which was originally involved in the C-terminal α-helix, as proposed on the basis of the conformation-dependent ^{13}C chemical shifts of intact preparation of [3-^{13}C]Ala-bR (*21–23*, *30*) of the intact preparation at 49.90 ppm, but inevitably changed to a random coil after cleavage at the site between Gly 231 and Glu 232 by papain, protruding from the membrane surface. On the other hand, the appreciably decreased peak resonating at 50.10 ppm on deletion of the terminal tail was ascribed to Ala 245 and 246 (Fig. 4F). At least three peaks (the highest-field peak at 47.96 ppm being assigned to Ala 235 prior to Pro, and those at 50.03 and 50.37 ppm to Ala 228 and 233 or *vice versa* from high to low field) remained in the CP-MAS spectrum when the C-terminus tail was digested by carboxypeptidase A, and the additional intense signal in the DD-MAS NMR spectrum was assigned to Ala 240 and 244. These findings were supported by the fact that the corresponding resonance position of the α-helix form is observed at lower field than the peak of the random coil form (50.1 ppm) at the boundary between the α-helix and β-sheet regions, and close to the data for the α-helix, as summarized in Table I.

Figure 5 illustrates the ^{13}C DD-MAS (A) spectrum of [1-^{13}C]Ala-labeled bR of the wild type, and CP-MAS (B–D) NMR spectra of A103C, A196G, and the wild type. The achieved spectral resolution of the transmembrane α-helices in the ^{13}C NMR signals of the Ala C=O group is again unexpectedly poor as compared with that of the Ala C_β group previously described (*29*). No appreciable spectral change was noted between A196G (and also A160G; spectrum not shown) and the wild type, in spite of the introduced site-directed mutations at the respective positions.

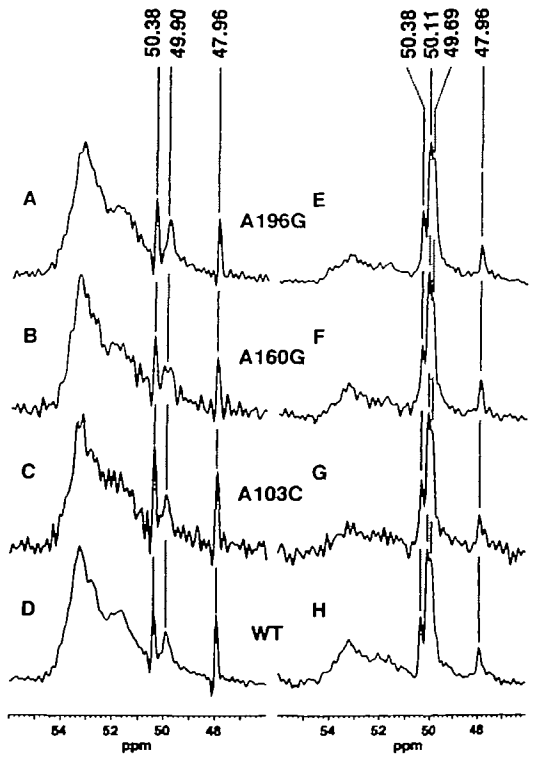

Fig. 3. **Comparison of ^{13}C CP-MAS (left) and DD-MAS (right) NMR spectra of [2-^{13}C]Ala-labeled bacteriorhodopsin (WT) and its site-directed mutants.**

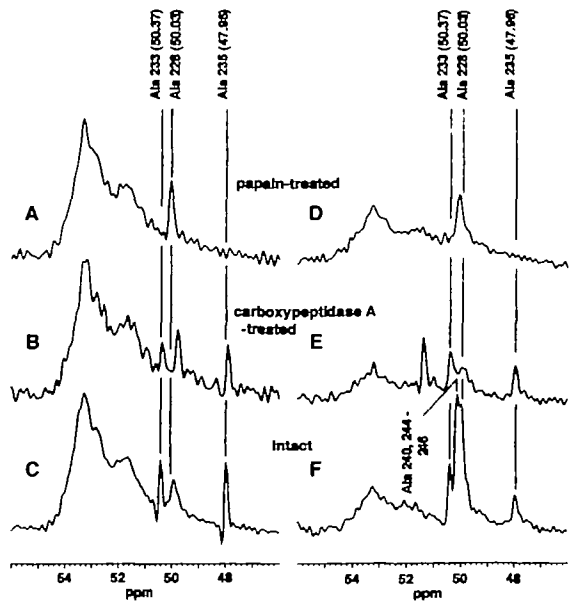

Fig. 4. **Variation of ^{13}C CP-MAS (left) and DD-MAS (right) NMR spectra of [2-^{13}C]Ala-labeled bacteriorhodopsin due to partial cleavage of the ^{13}C terminus by papain (A and D) and carboxypeptidase A (B and E), with reference to those of the intact protein (C and F).**

TABLE I. **^{13}C chemical shifts of the C-terminal α-helical domain protruding from the membrane surface (ppm from TMS).**

	Ala			Reference data[a]		
	233	228	235	α-helix	Random coil	β-sheet
C_α	50.38[b]	49.90[b]	47.96	52.4	50.1	48.2
C_β	15.91[c]	5.91[c]	17.20[c]	14.9	16.9	19.9
C=O	175.9[b]	175.6[b]	173.0	176.4	175.2	171.8

[a]Saitô, H., Tuzi, S., and Naito, A. (1998) *Annu. Rep. NMR Spectrosc.* **36**, 79–121; Saitô, H., Tuzi, S., Yamaguchi, S., Tanio, M., and Naito, A. (2000) *Biochim. Biophys. Acta* **1460**, 39–48. [b]Assignment interchangeable. [c]Tuzi, S., Yamaguchi, S., Tanio, M., Konishi, H., Inoue, S., Naito, A., Needleman, R., Lanyi, J.K., and Saitô, H. (1999) *Biophys. J.* **76**, 1523–1531.

This means that the carbonyl signals of Ala 196 and 160 in the F-G and E-F loops, respectively, were also completely suppressed for the wild type and these site-directed mutants, as in the case of [2-^{13}C]Ala-bR (Fig. 3), as mentioned above. However, a partially suppressed peak(s) is visible between the wild type and A103C mutant at the peak position around 174.0–174.2 ppm ascribable to the broad envelope of the Ala 103 signal (Fig. 5, B and D), because conformational flexibility of the shorter C-D loop might be restricted to some extent as compared with that of the longer E-F and F-G loops. This means that apparently resolved ^{13}C NMR signals in the loop region on CP-MAS NMR resonating at the peak positions between 173.0–175.9 ppm are not ascribable to the C-terminus, because no such signals were visible in the DD-MAS NMR spectrum (Fig. 5A).

In fact, the four well-resolved peaks visible in the DD-MAS NMR spectra could be ascribed to Ala residues located in the C-terminus (Fig. 5A), in a similar manner to that seen in the DD-MAS NMR spectrum of [2-^{13}C]Ala-bR (Fig. 2A). The highest-field peak resonating at 173.0 ppm can be unequivocally assigned to Ala 235 because of its location prior to the Pro residue by taking into account the expected upfield shift of the "proline effect" by 2–3 ppm (*31*), as confirmed in view of the sample cleaved by papain. Furthermore, the peaks at 175.9 and 175.6 ppm should be assigned to Ala 228 and 233 of the C-terminal α-helix, respectively, or *vice versa*. Undoubtedly, the most intense signals should be ascribed to Ala residues located at position 240 and beyond, as seen for the C_α peak in Fig. 2A.

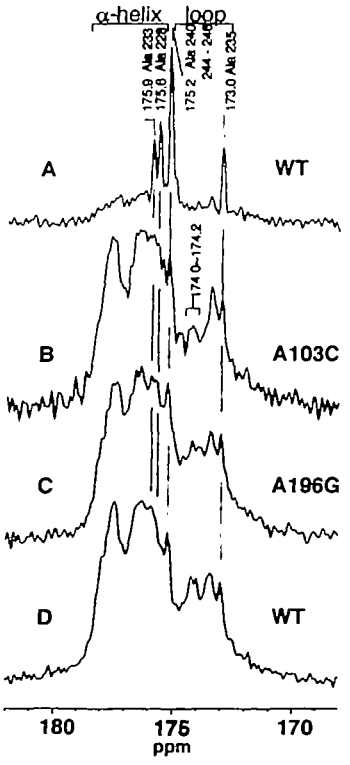

Fig. 5. **^{13}C DD-MAS (A) and CP-MAS (B–D) NMR spectra of [1-^{13}C]Ala-labeled bacteriorhodopsin.** Note that the peak intensity at 174.0–174.2 ppm of A103C (B) was partially suppressed as compared with that of the wild type (D).

These ^{13}C chemical shifts for the C-terminal α-helix are also summarized in Table I.

Furthermore, we recorded ^{13}C CP-MAS (upper traces) and DD-MAS NMR (lower traces) spectra of [1,2,3-$^{13}C_3$]Ala-bR, as illustrated in Fig. 6. Obviously, the spectral resolution is very poor as compared with that of the singly labeled spectra, as described above, except for the DD-MAS NMR spectrum of the carbonyl carbons. This is mainly caused by the presence of additionally split signals due to indirect spin-spin couplings and more seriously shortened spin-spin relaxation times on CP-MAS NMR, etc. Nevertheless, it was demonstrated that the four individual signals, as illustrated in Fig. 5A, were split into the doublet peaks due to indirect spin-spin couplings with the C_α carbon by 56 Hz. In contrast, no ^{13}C NMR signal was suppressed from the loop region of [3-^{13}C]Ala-bR, as mentioned already, and the resulting twelve ^{13}C NMR signals were well-resolved for both the CP-MAS (Fig. 7A) and DD-MAS NMR spectra at pH 7 with 10 mM NaCl (*29*). It turned out that increasing the ionic strength fivefold, *i.e.* from 10 mM to 50 mM NaCl, resulted in differential suppression of the ^{13}C NMR peak of the C-terminal α-helix (Ala 228 and 233 resonating at 15.89 ppm) and displaced the Ala 103 peak in the loop region. Furthermore, site-directed mutation of A160G in the E-F loop resulted in similar spectral modifications in the C-terminal α-helix and looped region in addition to the presence of a reduced peak at 16.40 ppm (Fig. 7C). The peak at 17.32 and the shoulder peak at 17.20 ppm are ascribed to Ala 184 (Tuzi *et al.*, to be published) and 235 (*25*), respectively.

We also recorded ^{13}C DD-MAS (upper traces) and CP-MAS (lower traces) NMR spectra of [1-^{13}C]Gly-bR (left) and a papain-cleaved preparation (right), as shown in Fig. 8, in order to determine how individual ^{13}C NMR peaks are resolved or suppressed depending on the region of interest. The major ^{13}C NMR signals of the Gly C=O group, as observed in the CP-MAS NMR spectra (Fig. 8B) in the region between 171.7–172.7 ppm, were unequivocally assigned to the transmembrane α-helices with reference to the data for the Gly residue involved in the α-helical segments of 14 Gly

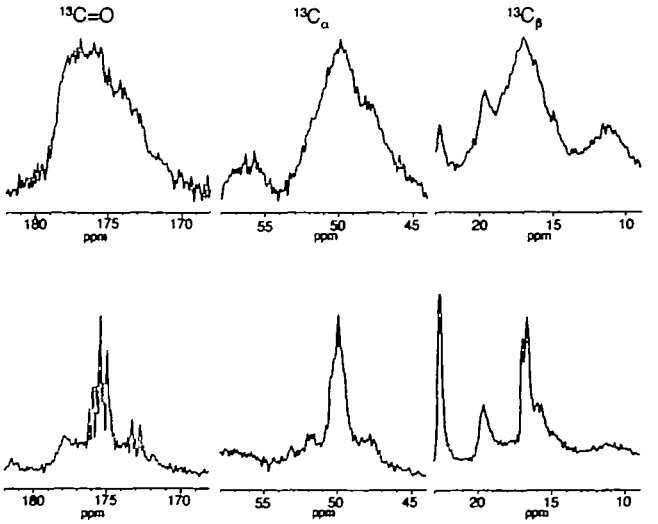

Fig. 6. **^{13}C CP-MAS NMR (upper traces) and DD-MAS NMR (lower traces) spectra of [1,2,3-$^{13}C_3$]Ala-bR.**

residues in the transmembrane α-helices. Naturally, the intense signal observed in the DD-MAS spectra at 171.7 ppm, which is absent for the papain-cleaved preparation, was ascribed to Gly 241 and 243 taking a random coil conformation as a result of their locations in the C-terminal tail. It appears, however, that the several peaks resonating at positions higher than 171.7 ppm should be ascribed to five Gly residues located in the loop region, although the assignment of the individual peaks is not feasible at present because of plausibly suppressed peaks from these regions. It is noteworthy that the center of gravity of the ^{13}C NMR signals of residues is displaced upfield by about of 3–4 ppm as compared with those of α-substituted amino acid residues due to natural abundance giving rise to a very broad envelope at 172.5 ppm.

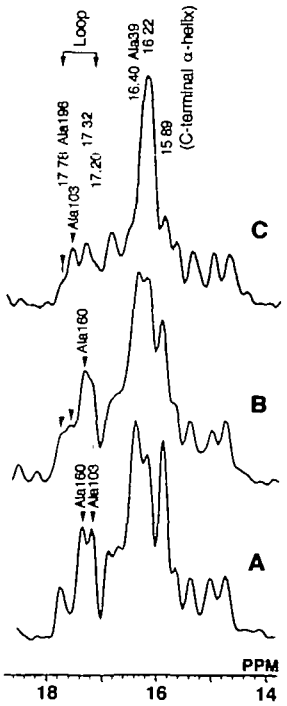

Fig. 7. **^{13}C CP-MAS NMR spectra of [3-^{13}C]Ala-bR with 10 mM NaCl (A) and 50 mM NaCl (B), and the [3-^{13}C]Ala-labeled A160G mutant with 10 mM NaCl (C).**

The carbon spin-lattice relaxation times in the laboratory frame (T_1^C) and spin-spin relaxation times under proton decoupling (T_2^C) of the above-mentioned samples were also measured by either the CP-MAS or DD-MAS NMR techniques, in order to distinguish the peaks of the C-terminus domains from those of the transmembrane α-helices and loops region in the former, as summarized in Tables II and III. As expected, the spin-lattice relaxation times for [1-^{13}C]Gly-, [1-^{13}C]- and [2-^{13}C]Ala-bR, as determined by CP-MAS NMR, are in the order of 20, 17–3, and 6–0.3 s, respectively, whereas those determined by DD-MAS NMR are in the order of 0.3 s, irrespective of their ^{13}C label. It is interesting to note that the spin-lattice relaxation times for the C-terminus, as determined in both the CP-MAS and DD-MAS NMR experiments, are in good agreement with each other, except for the peak at 50.03 ppm, which overlaps those of the C-terminal tail, as summarized in Table II. This means that the shortened carbon spin-lattice relaxation times are due to the C-terminal α-helical portion, which is able to undergo conformational fluctuations, as compared with those of loop regions. It is notable from Tables II and III that the observed T_2^C values for the transmembrane α-helix of [2-^{13}C]Ala-bR (3–5 ms) are rather

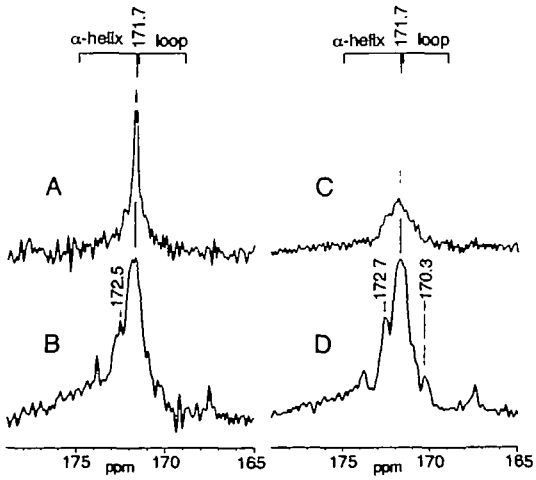

Fig. 8. **^{13}C DD-MAS (upper traces) and CP-MAS (lower traces) spectra of intact (left; A and B) and papain-cleaved (right; C and D) [1-^{13}C]Gly-labeled bacteriorhodopsin.**

TABLE II. **^{13}C spin-lattice relaxation times (T_1^C) (s) and spin-spin relaxation times under proton-decoupling and magic angle spinning (T_2^C) (ms) of [2-^{13}C]Ala-labeled bacteriorhodopsin.**

		Transmembrane α-helix		C-terminal α-helix			C-terminal end
		53.2 ppm	51.2 ppm	50.37 ppm (Ala 233)	50.03 ppm (Ala 228)	47.96 ppm (Ala 235)	50.1 ppm (Ala 240, 246–248)
T_1^C	CP-MAS	5.7 ± 1.7	9.0 ± 0.46	0.32 ± 0.17	1.1 ± 0.03	0.41 ± 0.23	
	DD-MAS			0.29 ± 0.03	0.32 ± 0.10	0.24 ± 0.05	0.32 ± 0.01
T_2^C	CP-MAS	2.8 ± 0.53	4.5 ± 0.17	9.4 ± 0.98	6.8 ± 0.05	17.3 ± 0.9	

TABLE III. **^{13}C spin-lattice relaxation times (T_1^C) (s) and spin-spin relaxation times under proton decoupling and magic angle spinning (T_2^C) (ms) of [1-^{13}C]Gly-, Val-, or Ala-labeled bacteriorhodopsin.**

		Gly		Val	Ala				
		α-helix		α-helix	α-helix		α-helix/random coil	C-terminus	
		172.7 ppm	171.8 ppm	174.2 ppm	177.5 ppm	176.5 ppm	175.9 ppm	175.2 ppm	173.0 ppm
T_1^C	CP-MAS	19.9 ± 1.7	24.1 ± 2.5	16.3 ± 2.8	16.8 ± 2.5			2.9 ± 0.21	8.3 ± 1.2
	DD-MAS		0.4 ± 0.04				1.76 ± 0.05	1.36 ± 0.05	1.43 ± 0.2
T_2^C	CP-MAS				7.2 ± 0.67	6.8 ± 0.67		13.3 ± 2.8	17.1 ± 2.8

short as compared with those of [1-^{13}C]Ala-bR (~7 ms). It is likely that such shortened T_2^C values for the loop region close to the T_2^C minimum may make the observation of signals difficult under the MAS conditions, as will be discussed in more detail later. In contrast, it appears that the longer T_2^C values for Ala residues located in the C-terminal α-helix arose from the correlation times around 10^{-6} s corresponding to the high-temperature side of the T_2^C minimum. This correlation time is still on the low temperature side, in the ^{13}C spin-lattice relaxation times of the laboratory frame, because the presence of such conformational fluctuation resulted in the decreased T_1^C values (Table II).

DISCUSSION

Confirmation of the C-Terminal α-Helix—Previously, Renthal *et al.* proposed the presence of a folded conformation on the cytoplasmic surface which undergoes conformational fluctuation in the order of ns on the basis of the results of a fluorescence probe experiment (*12*). Subsequently, we proposed that there is an α-helical segment in the C-terminal, protruding from the membrane surface, on the basis of the conformation-dependent displacement of the ^{13}C chemical shifts of [3-^{13}C]Ala-bR and proteolytic digestion of the C-terminal residues (*21–23, 30*). Consistent with these findings, the existence of an α-helical domain on the membrane surface of bR is now confirmed by the C_α and C=O ^{13}C chemical shifts of Ala 228 and 223 with reference to those of the α-helix form, as summarized in Table I, although the peak position of Ala 235 at the terminal end of this helix behaves as a turned structure because of its location prior to a Pro residue. The location of this α-helix protruding from the membrane surface is schematically indicated as helix G′ in Fig. 9. Otherwise, these ^{13}C NMR signals could be substantially broadened, as in most transmembrane α-helices (Fig. 2B). This view was further supported by its one order of magnitude shorter spin-lattice relaxation times (0.2–0.3 ms), reflecting a possible internal fluctuation, as compared with those of the transmembrane helices (5–10 s), as summarized in Table II. This sort of α-helix has not been found for bR so far by either X-ray diffraction or cryo-electron microscopic studies (*1–10*), probably because of the inherent disorder arising from conformational fluctuation of the order of 10^{-6} s, as estimated from the spin-lattice and spin-spin relaxation times discussed below, although a recent X-ray diffraction study on rhodopsin revealed the presence of a similar type of C-terminal α-helix protruding from the cytoplasmic surface (*32*).

Spectral Resolution—It turned out that the achieved spectral resolution of the ^{13}C CP-MAS NMR signals of the transmembrane α-helices of [1-^{13}C]-, [2-^{13}C]-, and [1,2,3-$^{13}C_3$]Ala- and [1-^{13}C]Gly-labeled bR and its mutants is far from satisfactory as compared with that for [3-^{13}C]Ala-bR previously reported (Figs. 2, 6, and 7) (*29*). Nevertheless, it is emphasized that the present finding is very valuable for the following two reasons, although they may be discouraging at first glance. This kind of information is very important as background knowledge for deciding what kind of strategy should be taken for future experimental design as to isotope-labeling to study more general membrane proteins, for instance, G-protein coupled receptor molecules. Furthermore, the correlation times of inherent fluctuations, if any, are unequivocally available from interference with either proton decoupling or magic angle spinning, without any kind of assumption as to the manner of molecular motions involved.

It is now not recommended, based on the data in Fig. 6, to prepare fully [^{13}C]Ala-labeled preparations when fully hydrated membrane proteins are to be fully examined, even if one wants increased spectral resolution for high-resolution NMR measurements (*23*). This is obviously caused by increased spin-spin relaxation pathways caused by various types of dipolar interactions among various types of ^{13}C-labeled nuclei and also split signals from ^{13}C-^{13}C homonuclear J couplings which can not be removed by either proton decoupling or magic angle spinning. Accordingly, no single carbon signal was resolved in the experiments utilizing these labels because of unexpectedly increased linewidths. This is not always true for [1-^{13}C]Val-labeled bR, however, because the ^{13}C NMR signals of Val 69 (B-C loop), 199 (F-G loop), and 49 (B helix) were well resolved (*33, 34*) in spite of their positions in the loop regions, probably because the acquired flexibility of these residues due to the presence of a Pro residue as the nearest neighbor may alter the motional frequency, thereby interfering with either proton decoupling or magic angle spinning.

The increased individual linewidths of the C_α and carbonyl carbons of Ala residue could be estimated from the observed spin-spin relaxation times under the condition of proton decoupling and magic angle spinning ($1/\pi T_2^C$), even though no single line was resolved due to the severe overlapping of many signals. They were estimated to be *ca.* 100 and 50 Hz (1 and 0.5 ppm), respectively, on the basis of the experimentally determined relaxation data summarized in Tables II and III. Again, it is well recognized that highly increased linewidths for the loop region made direct observation difficult. In contrast, the corresponding linewidths for [3-^{13}C]Ala-bR were determined from several single carbon signals to be 20–25 Hz after resolution enhancement by Gaussian multiplication. Therefore, it was concluded that [3-^{13}C]Ala-labeling is more suitable than [1-^{13}C]-, [2-^{13}C]-, and [1,2,3-$^{13}C_3$]Ala- and [1-^{13}C]Gly-labeling as far as the ^{13}C NMR signals of the transmembrane α-helices and loops are concerned. It was further demonstrated that more detailed argument as to the significance of the α_{II}-helix in an anisotropic membrane environment was made possible (*35, 36*) once well-resolved signals from different residues were resolved, although such argument was partly feasible on the basis of the carbonyl signals.

In contrast, the spectral resolution for the peaks of the C-terminus residues in the DD-MAS NMR spectrum turned out to be much better for [1-^{13}C]- and [2-^{13}C]Ala-labeling in view of their larger spectral separations of 2.9 and 2.4 ppm, respectively, as compared with that of 1.91 ppm for [3-^{13}C]Ala-bR. In fact, the expected linewidths for these residues range from 2 to 30 Hz, as estimated from the observed spin-spin relaxation times under proton decoupling listed in Tables II and III. In addition, it is expected that the observed changes in the spin-lattice and spin-spin relaxation times for [1-^{13}C]- and [2-^{13}C]Ala-bR could be more directly related to the changes in backbone motion, as will be discussed below, while these relaxation parameters of [3-^{13}C]Ala-bR are influenced by the presence of C_3 rotation of the methyl groups rather than the backbone motions under consideration.

Surface Dynamics of the Loop and C-Terminus Helix—The present findings shown in Fig. 7 indicate that the C-terminal α-helix (G′ helix in Fig. 9) is linked together with the cytoplasmic loops to form a surface structure through the formation of cation-mediated linkages (or salt bridges) between their positively or negatively charged side-chains, because this surface structure was disrupted by increased ionic strength (50 mM) to compete with bound divalent cations (Fig. 7B) or conformational modification of the E-F loop (Fig. 7C) through introduction of site-directed mutagenesis at this site. This situation is most obviously indicated by the decreased peak-intensities of the C-terminal α-helix on CP-MAS NMR (but not on DD-MAS) as a result of the acquired conformational flexibility (with a correlation time of the order of 10^{-8} s) caused by disruption of such linkages. More detailed characterization of the local motions in bR is also feasible through measurements of spin-lattice or spin-spin relaxation parameters, which are sensitive to fast and slow motions, respectively, with different correlation times, in addition to the arguments based on the specific suppression of peaks. In particular, longer carbon spin-lattice relaxation times in the laboratory frame of the C-terminal tail can be conveniently utilized to detect rapid (or isotropic) motions with correlation times of shorter than 10^{-8} s. This can be very easily visualized when the T_1^C values of [2-^{13}C]Ala-bR for the transmembrane α-helices (8–20 s), as determined in the CP-MAS experiments, were compared with those of the C-terminus residues (0.3–1.8 s), as determined by DD-MAS experiments (Tables II and III). The correlation times of the latter may be located at the T_1^C minimum or on the high-temperature side when combined with measured T_2^C values, whereas those of the former are on the low temperature side of the T_1^C minimum. Obviously, the ^{13}C NMR signal in the CP-MAS experiment could be suppressed when the local motions responsible for this type of relaxation are on either isotropic or large-amplitude reorientation, as for the terminal tail of the C-terminus.

Carbon spin-spin relaxation times (T_2^C) under CP-MAS conditions can provide motional information about the *individual carbon* sites of amino acid residues of interest, in contrast to the case of proton spin-lattice relaxation times in the rotating frame ($T_{1\rho}^H$) (*20*, *21*), in which information on individual sites would be masked by the presence of the rapid spin-spin process. Indeed, we have already noticed that the T_2^C values for the C-terminal α-helix, which is capable of undergoing more rapid motion, are appreciably higher than those from the transmembrane α-helices, as demonstrated in Tables II and III. In general, the T_2^C value strongly depends on the ^{1}H decoupling field intensity, and is affected by interference between incoherent random motion and coherent decoupling and spinning frequencies. Therefore, the overall $1/T_2^C$ can be given by (*24*, *28*)

$$1/T_2^C = (1/T_2^C)^S + (1/T_2^C)^M_{DD} + (1/T_2^C)^M_{CS} \quad (1)$$

$$(1/T_2^C)^M_{dd} = \Sigma(4\gamma_I^2\gamma_S^2\hbar^2/15r^6)I(I+1)(\tau_c/(1+\omega_I^2\tau_C^2)) \quad (2)$$

$$(1/T_2^C)^M_{CS} = \Sigma(\omega_0^2\eta^2\delta^2/45)[\tau_c/(1+4\omega_r^2\tau_c^2) + 2\tau_c/(1+\omega_r^2\tau_c^2)], \quad (3)$$

where $(1/T_2^C)^S$ is the transverse component due to the C–H static dipolar interaction. Here, γ_I and γ_S are the gyromagnetic ratios of S (^{13}C observed) and I (^{1}H or ^{13}C) nuclei, respectively, r is the internuclear distance between spins I and S, and the summation is over each ^{13}C nuclei or either ^{13}C–H or ^{13}C–^{13}C pairs. ω_0 and ω_I are the carbon resonance frequency and the amplitude of the proton decoupling RF field, respectively. ω_r is the angular velocity of spinner rotation. δ is the chemical shift anisotropy and η is the asymmetric parameter of the chemical shift tensor. Clearly, the transverse relaxation rate is dominated by modulation of either dipolar interactions or chemical shift anisotropies, if internal fluctuations cannot be ignored as in the cases of membrane proteins. It is expected that a decoupling of 50 kHz is sufficient to reduce the static component and the $(1/T_2^C)^M_{CS}$ term will be dominant in the overall $1/T_2^C$, as far as the carbonyl carbons with larger chemical shift anisotropies are concerned. In addition, it is expected that the C_α carbon signal could also be affected by both the $(1/T_2^C)^M_{DD}$ and $(1/T_2^C)^M_{CS}$ terms, depending upon the frequency range of either 50 kHz (ω_I) or 4 kHz (ω_r), respectively. It has been demonstrated that the T_2^C minimum could be located at the correlation time of 10^{-5} s or 10^{-4} s, depending on the dominant mechanism either from the dipole-dipole interaction (DD; Eq. 2) or chemical shift anisotropy (CS: Eq. 3), respectively.

It appears, on the basis of the aforementioned argument, that the correlation times of the C-terminal α-helix, from which appreciably higher T_2^C values than those of the transmembrane α-helices were observed, are definitely on the higher temperature side of the T_2^C minimum, which could be close to 4 kHz (spinner frequency), as demonstrated by Eq. 2. The absence of peaks for the interhelical loops is thus ascribed to the correlation times corresponding to the T_2^C minimum of the chemical shift anisotropy mechanism (Eq. 3). In this connection, it is interesting to note that the carbonyl ^{13}C signal of the Ala 103 residue located in the shorter C-D loop was partially suppressed, while those of Ala 160 and 196 located in the longer E-F and F-G loops were completely suppressed (Fig. 6), consistent with the previous observation on heavy-atom labeling with an X-ray projection map (*16*): the heavy-atom positions of residues 101 (C-D loop) and 130 (D-E loop) were determined, while residues 160 (E-F loop) and 231 (C-terminus) could not be located. As previously demonstrated (*30*, *37*), the transmembrane α-helices of bR are involved in local conformational fluctuation of low frequency, especially in an anisotropic environment such as lipid bilayers, resulting in downfield displacement of the peaks by 1–2 ppm from those of the normal α-helix, and have been characterized as α_{II} helices with reference to the peak-positions of ^{13}C chemical shifts of $(Ala)_n$ in a hexafluoroisopropanol (HFIP) solution, according to the definition of Krimm and Dwivedi based on IR measurements (*36*). A similar result was very recently obtained for a variety of chemically synthesized transmembrane peptides incorporated into lipid bilayers (*35*). The time-scale of such motion, if any, could be faster than 10^2 Hz (correlation time in the order of 10^{-2} s) (*37*) as viewed from the chemical exchange process of chemical shift among various conformations undergoing slow anisotropic fluctuation, as schematically depicted in Fig. 9. As a result, any observed ^{13}C chemical shift δ, especially from [3-^{13}C]Ala-bR, can be expressed as a time-averaged value from various conformers undergoing chemical exchange faster than the chemical shift difference (δ_i) among the various peaks for various substrates, instead of the static picture so far anticipated, as follows

$$\delta = \Sigma p_i \delta_i \quad (4)$$

$$\Sigma p_i = 1 \quad (5)$$

where p_i stands for the population for the respective substrates. It is therefore very important to estimate these parameters in order to obtain a more detailed picture of membrane proteins.

Biological Significance of Surface Dynamics—It is now clear that the dynamic aspects of bR are highly heterogeneous depending upon the respective domains, with distribution of the correlation times from 10^{-2} s of the transmembrane α-helices to 10^{-8} s of the C-terminal tail (Fig. 9). From this picture, it is readily conceivable that the abovementioned motionally different domains, the cytoplasmic loops (10^{-4} s) and C-terminal α-helix (10^{-6} s), are linked together through the formation of cation-mediated linkages or salt bridges between charged side-chains. It was demonstrated previously that the F-G loop and some transmembrane α-helices of bacterio-opsin (bO) (*23*) acquired accelerated motional freedom with approximate correlation times of 10^{-5} s, compared with those of 10^{-4} and 10^{-2} s for bR, respectively, as judged from the suppressed peaks in both the CP-MAS and DD-MAS spectra, when retinal is removed from bR. Recently, a similar spectral change was also observed for an M-like state achieved by the D85N mutant without photo-illumination at ambient temperature (*38*). It appears that these kinds of conformational changes as well as fluctuation are necessary for the entry of retinal into bO to form bR or a conformational switch resulting in the next steps in photocycles for the M state. In other words, the presence of the intrinsic flexibility (10^{-4} s) and subsequent susceptibility to further change of the loops in bR seems to be essential for the coming large amplitude motions of the transmembrane α-helices in the conformational switch immediately after the deprotonation of Schiff base. In this connection, it is particularly interesting that the surface structure of bR in the M-like state is largely reorganized, depending upon the ionization state at both Asp 85 and the Schiff base located in an inner site of the membrane (*38*), to facilitate the proton uptake in the cytoplasmic surface more effectively. Recently, it was also pointed out, on the basis of the results of a neutron scattering experiment, that this time-scale is related to a number of conformational change or protein–protein interactions during a number of important biological processes (*39*). In this connection, it appears that further work along these lines is very important, in order to understand the molecular process underlying the signal transduction in G-protein coupled receptors.

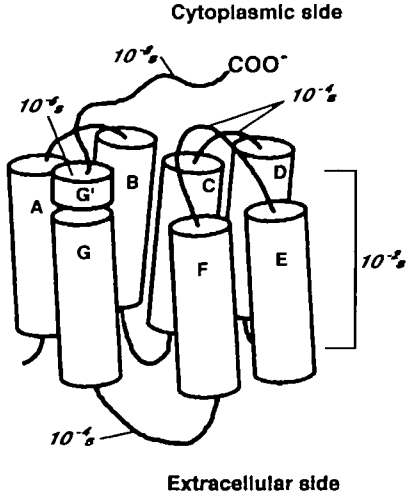

Fig. 9. **Schematic representation of the location of the C-terminal α-helix (helix G′ protruding from the membrane surface) and heterogeneity of the approximate correlation times of the different domains, as estimated from specifically suppressed peaks by comparative studies involving CP-MAS and DD-MAS NMR measurements, the carbon spin-lattice relaxation times and spin-spin relaxation times under CP-MAS conditions, and the chemical exchange process.**

REFERENCES

1. Henderson, R., Baldwin, J.M., Ceska, T.A., Zemlin, F., Beckman, E., and Downing, K.H. (1990) Model for the structure of bacteriorhodopsin based on high-resolution electron cryo-microscopy. *J. Mol. Biol.* **213**, 899–929
2. Grigorieff, N., Beckmann, E., and Zemlin, F. (1995) Lipid location in deoxycholate-treated purple membrane at 2.6 Å. *J. Mol. Biol.* **254**, 404–415
3. Kimura, Y., Vassylyev, D.G., Miyazawa, A., Kidera, A., Matsushima, K., Mitsuoka, K., Murata, K., Hirai, T., and Fujiyoshi, Y. (1997) Surface of bacteriorhodopsin revealed by high-resolution electron crystallography. *Nature* **389**, 206–211
4. Pebay-Peyroula, E., Rummel, J.P., Rosenbusch, J.P., and Landau, E.M. (1997) X-ray structure of bacteriorhodopsin at 2.5 angstroms from microcrystals grown in lipidic cubic phases. *Science* **277**, 1676–1681
5. Luecke, H., Richter, H.T., and Lanyi, J.K. (1998) Proton transfer pathways in bacteriorhodopsin at 2.3 angstrom resolution. *Science* **280**, 1934–1937
6. Essen, L., Siegert, R., Lehmann, W.D., and Oesterhelt, D. (1998) Lipid patches in membrane protein oligomers: crystal structure of the bacteriorhodopsin-lipid complex. *Proc. Natl. Acad. Sci. USA* **95**, 11673–11678
7. Luecke, H., Schobert, B., Richter, H.-T., Cartailler, J.-P., and Lanyi, J.K. (1999) Structure of bacteriorhodopsin at 1.55 Å resolution. *J. Mol. Biol.* **291**, 899–911
8. Belrhali, H., Nollert, P., Royant, A., Menzel, C., Rosenbusch, J.P., Landau, E.M., and Pebay-Peyroula, E. (1999) Protein, lipid and water organization in bacteriorhodopsin crystals: a molecular view of the purple membrane at 1.9 Å resolution. *Structure Fold Des.* **7**, 909–917
9. Luecke, H., Schobert, B., Richter, H.T., Cartailler, J.P., and Lanyi, J.K. (1999) Structural changes in bacteriorhodopsin during ion transport at 2 angstrom resolution. *Science* **286**, 255–261
10. Edman, K., Nollert, P., Royant, A., Belrhali, H., Pebay-Peyroula, E., Hajdu, J., Neutze, R., and Landau, E.M. (1999) High-resolution X-ray structure of an early intermediate in the bacteriorhodopsin photocycle. *Nature* **401**, 822–826
11. Liao, M.J. and Khorana, H.G. (1984) Removal of the carboxyl terminal peptide does not affect refolding or function of bacteriorhodopsin as a light-dependent proton pump. *J. Biol. Chem.* **259**, 4194–4199
12. Renthal, R., Dawson, N., Tuley, J., and Horowitz, P. (1983) Constraints on the flexibility of bacteriorhodopsin's carboxyl terminal tail at the purple membrane surface. *Biochemistry* **22**, 5–12
13. Marque, J., Kinoshita, K.J., Govindjee, R., Ikegami, A., Ebrey, T.G., and Otomo, J. (1986) Environmental modulation of C-terminus dynamic structure in bacteriorhodopsin. *Biochemistry* **25**, 5555–5559
14. Steinhoff, H.J., Mollaaghababa, R., Altenbach, C., Hideg, K., Krebs, M., Khorana, H.G., and Hubbell, W.L. (1994) Time-resolved detection of structural changes during the photocycle of spin-labeled bacteriorhodopsin. *Science* **266**, 105–107

15. Krebs, M.P., Behrens, W., Mollaaghababa, R., Khorana, H.G., and Heyn, M.P. (1993) X-ray diffraction of a cysteine-containing bacteriorhodopsin mutant and its mercury derivative. Localization of an amino acid residue in the loop of an integral membrane protein. *Biochemistry* **32**, 12830–12834
16. Behrens, W., Alexiev, U., Mollaaghababa, R., Khorana, H.G., and Heyn, M.P. (1998) Structure of the interhelical loops and carboxyl terminus of bacteriorhodopsin by X-ray diffraction using site-directed heavy-atom labeling. *Biochemistry* **37**, 10411–10419
17. Saitô, H. (1986) Conformation-dependent ^{13}C chemical shifts: a new means of conformational characterization as obtained by high-resolution solid-state NMR. *Magn. Reson. Chem.* **24**, 835–852
18. Saitô, H. and Ando, I. (1989) High-resolution solid-state NMR studies of synthetic and biological macromolecules. *Annu. Rep. NMR Spectrosc.* **21**, 209–290
19. Saitô, H., Tuzi, S., and Naito, A. (1998) Empirical versus non-empirical evaluation of secondary structure of fibrous and membrane protein by solid-state NMR: a practical approach. *Annu. Rep. NMR Spectrosc.* **36**, 79–121
20. Tuzi, S., Naito, A., and Saitô, H. (1993) A high-resolution solid-state ^{13}C-NMR study on [1-^{13}C]Ala and [3-^{13}C]Ala and [1-^{13}C]Leu and Val-labelled bacteriorhodopsin. Conformation and dynamics of transmembrane helices, loops and termini, and hydration-induced conformational change. *Eur. J. Biochem.* **218**, 837–844
21. Tuzi, S., Yamaguchi, S., Naito, A., Needleman, R., Lanyi, J.K., and Saitô, H. (1996) Conformation and dynamics of [3-^{13}C]Ala-labeled bacteriorhodopsin and bacterioopsin, induced by interaction with retinal and its analogs, as studied by ^{13}C nuclear magnetic resonance. *Biochemistry* **35**, 7520–7527
22. Yamaguchi, S., Tuzi, S., Seki, T., Tanio, M., Needleman, R., Lanyi, J.K., Naito, A., and Saitô, H. (1998) Stability of the C-terminal α-helical domain of bacteriorhodopsin that protrudes from the membrane surface, as studied by high-resolution solid-state ^{13}C NMR. *J. Biochem.* **123**, 78–86
23. Saitô, H., Tuzi, S., Yamaguchi, S., Tanio, M., and Naito, A. (2000) Conformation and backbone dynamics of bacteriorhodopsin revealed by ^{13}C NMR. *Biochim. Biophys. Acta* **1460**, 39–48
24. Rothwell, W.P. and Waugh, J.S. (1981) Transverse relaxation of dipolar coupled spin system under rf irradiation: detecting motions in solid. *J. Chem. Phys.* **75**, 2721–2732
25. Yamaguchi, S., Tuzi, S., Tanio, M., Naito, A., Lanyi, J.K., Needleman, R., and Saitô, H. (2000) Irreversible conformational change of bacterio-opsin induced by binding of retinal during its reconstitution to bacteriorhodopsin, as studied by ^{13}C NMR. *J. Biochem.* **127**, 861–869
26. Onishi, H., McCance, M.E., and Gibbson, N.E. (1965) A synthetic medium for extremely halophilic bacteria. *Can. J. Microbiol.* **11**, 365–373
27. Oesterhelt, D. and Stoeckenius, W. (1974) Isolation of the cell membrane of *Halobacterium halobium* and its fractionation into red and purple membrane. *Methods Enzymol.* **31**, 667–678
28. Naito, A., Fukutani, A., Uitdehaag, M., Tuzi, S., and Saitô, H. (1998) Backbone dynamics of polycrystalline peptides studied by measurements of ^{15}N NMR lineshapes and ^{13}C transverse relaxation times. *J. Mol. Struct.* **441**, 231–241
29. Tuzi, S., Yamaguchi, S., Tanio, M., Konishi, H., Inoue, S., Naito, A., Needleman, R., Lanyi, J.K., and Saito, H. (1999) Location of a cation-binding site in the loop between helices F and G of bacteriorhodopsin as studied by ^{13}C NMR. *Biophys. J.* **76**, 1523–1531
30. Tuzi, S., Naito, A., and Saito, H. (1994) ^{13}C NMR study on conformation and dynamics of the transmembrane α-helices, loops, and C-terminus of [3-^{13}C]Ala-labeled bacteriorhodopsin. *Biochemistry* **33**, 15046–15052
31. Wishart, D.S., Sykes, B.D., and Richards, F.M. (1991) Relationship between nuclear magnetic resonance chemical shift and protein secondary structure. *J. Mol. Biol.* **222**, 311–333
32. Palczewski, K., Kumasaka, T., Hori, T., Behnke, C.A., Motoshima, H., Fox, B.A., Le Trong, I., Teller, D.C., Okada, T., Stenkamp, R.E., Yamamoto, M. and Miyano, M. (2000) Crystal structure of rhodopsin: a G-protein-coupled receptor. *Science* **289**, 739–745
33. Tanio, M., Inoue, S., Yokota, K., Seki, T., Tuzi, S., Needleman, R., Lanyi, J.K., Naito, A., and Saitô, H. (1999) Long-distance effects of site-directed mutations on backbone conformation in bacteriorhodopsin, from solid state NMR of [1-^{13}C]Val-labeled proteins. *Biophys. J.* **77**, 431–442
34. Tanio, M., Tuzi, S., Yamaguchi, S., Kawaminami, R., Naito, A., Needleman, R., Lanyi, J.K., and Saitô, H. (1999) Conformational changes of bacteriorhodopsin along the proton-conduction chain as studied with ^{13}C NMR of [3-^{13}C]Ala-labeled protein: Arg 82 may function as an information mediator. *Biophys. J.* **77**, 1577–1584
35. Kimura, S., Naito, A., Tuzi, S., and Saitô, H. (2001) A ^{13}C NMR study on [3-^{13}C]-, [1-^{13}C]Ala- or [1-^{13}C]Val-labeled transmembrane peptides of bacteriorhodopsin in lipid bilayers: insertion, rigid-body motions and local conformational fluctuations at ambient temperature. *Biopolymers* **58**, 78–88
36. Krimm, S. and Dwivedi, A.M. (1982) Infrared spectrum of the purple membrane: clue to proton conduction mechanism? *Science* **216**, 407–408
37. Tuzi, S., Naito, A., and Saitô, H. (1996) Temperature-dependent conformational change of bacteriorhodopsin as studied by solid-state ^{13}C NMR. *Eur. J. Biochem.* **239**, 294–301
38. Kawase, Y., Tanio, M., Kira, A., Yamaguchi, S., Tuzi, S., Naito, A., Kataoka, M., Lanyi, J.K., Needleman, R., and Saitô, H. (2000) Alteration of conformation and dynamics of bacteriorhodopsin induced by protonation of Asp 85 and deprotonation of Schiff base as studied by ^{13}C NMR. *Biochemistry* **39**, 14472–14480
39. Zaccai, G. (2000) How soft is a protein? A protein dynamics force constant measured by neutron scattering. *Science* **288**, 1604–1607